

**Title of the manuscript****Synergy between magneto-rheological fluids and aluminum foams.****Prospective alternative for seismic damping****Authors:**

M. Aguilera Portillo<sup>1</sup>, P. Santa Ana Lozada<sup>1</sup>, I.A. Figueroa<sup>2</sup>,  
M.A. Suárez<sup>2</sup>, A.V. Delgado<sup>3</sup>, G.R. Iglesias<sup>3</sup>

*<sup>1</sup>Master and Doctoral Programmes in Architecture*

*and*

*<sup>2</sup>Institute of Materials Research.*

*National Autonomous University of Mexico. Mexico DF*

*<sup>3</sup>Department of Applied Physics, School of Science, University of Granada.*

*18071 Granada, Spain*

**Corresponding author:**

G.R. Iglesias

Department of Applied Physics

School of Sciences

University of Granada, 18071 Granada, Spain

e-mail: iglesias@ugr.es

**Abstract**

This article presents the experimental study of a preliminary investigation of a seismic damper device aimed at improving the behavior of structures when subjected to earthquakes. The damper is the result of a binomial material formed by aluminum foam with pores 1 mm in diameter, wetted by a magnetorheological fluid (MRF). The objective of the present work is to explore the synergy between the two components in a magnetorheological test, and to evaluate the effect of the Al foam pores in the structure buildup of the fluid. The analysis is completed with a compressive test carried out on the MRF-filled foam in the presence of a magnetic field. This kind of test demonstrates that the deformation of the foam for very small loads is limited by the hardening of the fluid because of its MR response. The results of this research suggest that there is a mutual benefit between the components of the device, presumably leading to an enhanced dissipation of vibration energy.

**Keywords:** Magneto-rheological fluid; dissipation of energy; seismic damper; metal foam; magnetorheological analysis



## INTRODUCTION

A magnetorheological fluid (MRF) is a kind of intelligent material typically in the form of a complex fluid with a high concentration of magnetizable microparticles dispersed in a non-magnetic fluid (Bossis et al., 2002; Carlson and Jolly, 2000; de Vicente et al., 2011; Lopez-Lopez et al., 2006; Velte et al., 2011). Other formulations, including mixed micro- and nano-particles, or non-magnetic holes in a ferrofluid (Rodriguez-Arco et al., 2014), are possible, but not so generally used in applications. Its name comes, in any case, from the fact that the application of an often homogeneous magnetic field produces an increase of the apparent viscosity of the suspension, and a modification of its rheological behavior from Newtonian to viscoelastic, with yield stress or elastic modulus up to 100 kPa (Pradeep P. Phulé, 1999). These changes occur in a few ms and are removed reversibly when the magnetic field is switched off (Baranwal and Deshmukh, 2008; Chacón Hernando, 2009). This rheological ability to control the structure is due to well-defined particle chain structures formed by the alignment of the magnetic moments of the particles in the field direction (Furst and Gast, 2000).

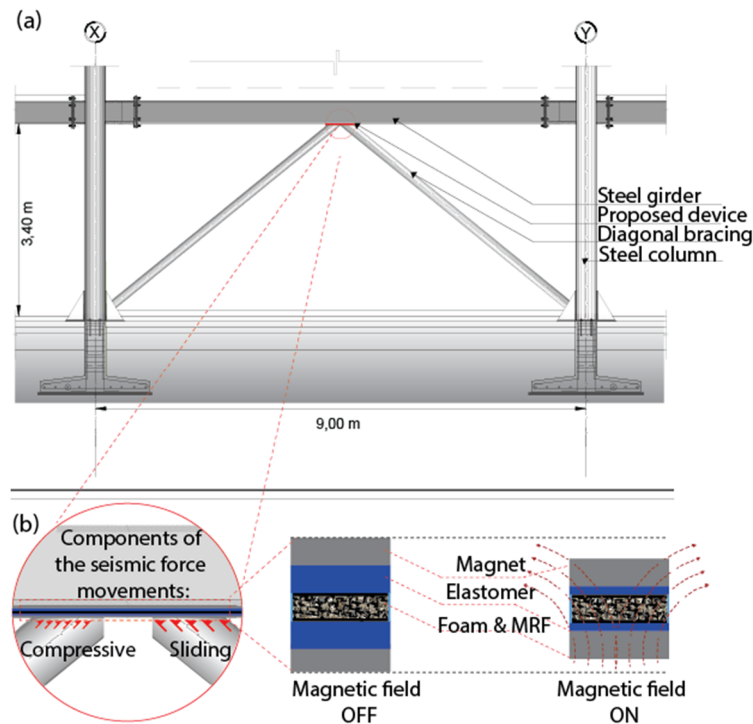
The strength of the magnetorheological effect is directly related to the amount, size distribution, shape, density, saturation magnetization and coercivity of the magnetic particles in the suspension, as well as to the strength of the magnetic field applied. The dispersed phase can be either a ferri- or ferromagnetic material, usually consisting of soft magnetic particles, including iron, magnetite, or other ferrites (Carlson and Jolly, 2000).

Since their discovery in the 1940's, the application of magnetorheological suspensions has forged its way into several branches of technological development including such industrial areas as aerospace (Bong Jun Park, 2010), biomedical prostheses, drug vehicles design (Rudzka et al., 2013), and mechanical engineering. In the latter, brakes, shock absorbers, vibration controllers, dampers and seismic insulators (Bhatti, 2012; Eem et al., 2013; Gordaninejar et al., 2010; Rossa et al., 2014a; Rossa et al., 2014b) have been devised.

In the particular field of architecture, the importance of the design of light and resistant materials that provide damping is a continuous need. Inspired by natural cellular materials, either metallic or polymeric foams have been designed which are capable of dissipating strain energy when subjected to mechanical vibration under cyclic deformation (Banhart, 2001; Fusheng et al., 1999). Recently, there have been

proposals of MR dampers aiming at these applications, based on the incorporation of metallic foams as support for the MRF (Carlson, 1999; Liu, 2010; Liu et al., 2010; Yan et al., 2013). The MRF in this case would be confined in the foam without the need of expensive, degradable seals, and as a result these devices may become a good option for low-cost absorbers production.

Based on above, in this work it is proposed the design and mechanical analysis of a seismic impact-absorbing device, using the MR effect in a composite system formed by an aluminum foam filled with a magnetorheological fluid. The final aim of the project would be to build a panel for steel structures from 1 to 6 story frames, so as to improve protection during an earthquake. A first step is the study of the synergy between the MRF and an aluminum foam with highly interconnected pores. This will be carried out at the laboratory scale, starting from the evaluation of the magnetorheological response of the composite structure. The research methodology used was based on the *Technology Readiness Level* as instrument for the creation and incorporation of products in the market. Ideally, the MR foam could be implemented in a structure as illustrated in Figure 1. A common method to increase the stiffness of structural frames is the addition of diagonal braces. In order to design earthquake-resisting buildings, engineers propose the incorporation of energy dissipating devices, at the joint with the steel gilder, (Figure 1a) such as ADAS or TADAS metallic dampers (Hosseini and Farsangi, 2012). This kind of devices, absorb and dissipate energy during earthquakes, due to the movement of the upper end of the passive device, relative to the lower end, which causes yielding of the plates composing it. This location has great concentration of displacement, which causes shear stress in the building materials. As shown in Figure 1b, the MRF-foam device is proposed also in a passive configuration: a pair of magnets will confine the MRF in the foam, and when the seismic wave goes in the structure, the magnet approaches the foam inducing the magnetorheological effect, this hampering the movement from the diagonal bracing to the steel gilder, reducing the amount of seismic energy to be dissipated in the upper story frames of the structure.



**Figure 1.** (a) Theoretical location of the energy dissipating devices in the architecture-structural system. (b) Details of the operation: configurations in field-off and field-on conditions.

## Experimental

### *Aluminum foam elaboration: metal infiltration method*

The infiltration method consists in the casting and injection of a molten metal in a preform, and it can be applied to a large variety of metals (Figuroa Vargas et al., 2012). In our case the foams were made from industrial aluminum (Alfa Aesar, Mexico), with 99.9% purity and density  $2.7 \text{ g/cm}^3$ . This selection was made because of its diamagnetic behavior, low cost, abundance on earth's surface, easy recyclability and high stiffness, in combination with a comparatively low density (Gutiérrez-Vázquez and Oñoro, 2008).

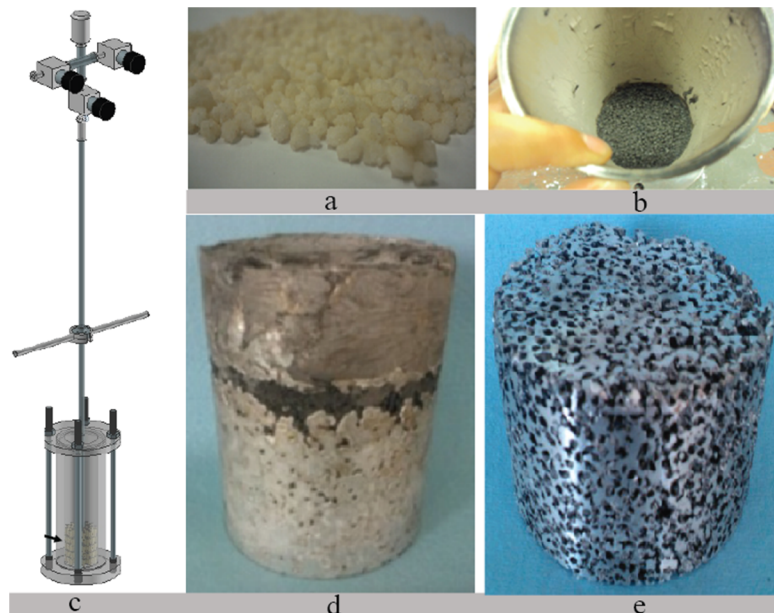
The procedure was performed in the following steps:

1. For the pellet preparation, a mixture containing 22 % (by weight) water, 68 % NaCl and 10 % flour was prepared until a consistent dough was obtained, capable of spreading spontaneously. A 1 cm thick layer was produced, dried at ambient conditions for 2 days and ground to the desired size (approximately 1 mm) in a mortar.

2. The pellets (total 415 g) were poured in a cylindrical, stainless steel 316 crucible, 27 cm high and 10 cm in outer diameter. The crucible was heated during 1 hour in a pre-heated furnace at 200°C. After this extensive drying, the preform was calcined at 350°C during 30 min.
3. 700 to 1000 g aluminum was placed on top of the preform and a vacuum of  $5.5 \times 10^{-2}$  Torr was produced under an Ar protective atmosphere which was maintained while the crucible was placed in the furnace now preheated at 600 to 750°C, depending on the required interconnectivity.
4. The final cylindrical foams were 5 mm in height and 2.54 cm in diameter. Two kinds of preparations were selected for the present study, as detailed in Table 1. Figure 2 shows the different steps in the preparation.

**Table 1.** Samples selected for the MR damper study.

Sample	Dough mass (g)	Density (g/cm <sup>3</sup> )	Porosity (%)
1	2.52	0.9968	63
2	2.12	0.8415	69



**Figure 2.** Illustration of the different steps of the Al foam preparation. a) Untreated pellets; b) dried and calcined pellets; c) controlled-atmosphere crucible; d) resulting foam; e) the same after cleaning with water and ultrasounds.

### *MRF preparation*

HQ carbonyl iron powder from BASF (Germany) was used as solid phase. It consists of spherical particles with a median particle size of  $d_{50} = 2.3 \mu\text{m}$  (particle diameters range from 0.5 to 3  $\mu\text{m}$ ) and an iron content of 97% (density = 7.5  $\text{g}/\text{cm}^3$ ). The base carrier fluid was mineral oil (Sigma Aldrich) and it was used for all the suspensions; its viscosity at 25 °C is (0.028  $\pm$  0.001) Pa·s. The solids concentrations used were 25, 30, 35, 40 and 45% v/v. Additives for stabilizing the particles were incorporated as described in (Durán et al., 2008).

The MR characterization of the fluids tested was carried out in an MCR300 Rheometer from Physica-Anton Paar (Austria), provided with a Magneto-Rheological Device (Physica MRD). The magnetic circuit is designed so that the magnetic flux lines are normal to the parallel disks. A parallel plate (20 mm in diameter) configuration was used, with a 7 mm gap. This is rather large, but was necessary because of the thickness of the Al foam disks supporting the fluids. In the manufacturer's design, a yoke covering the upper plate allows for a quite homogenous magnetic field through the sample volume. With the modification necessary for our tests, the yoke was placed 5 mm above its normal working position. Because in such configuration the homogeneity of the field might be compromised, we measured its normal component using a GM08 gaussmeter from Hirst Magnetic Instruments Ltd. (UK), with a 100  $\mu\text{T}$  resolution. In our case the maximum variation of the field along the diameter was less than 5 %, and vertically along the axis it was 10 % at most. Thus, although the homogeneity is partially sacrificed, the results are still meaningful in the context of this investigation. In order to keep the fluid in a fixed position, we used a thin plastic container surrounding the foam and fluid film. The bottom plate of the MRF is the aluminum foam piece, with very rough surface. The top plate is serrated to avoid wall slip.


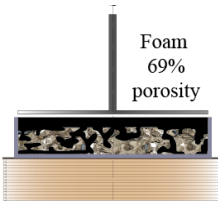
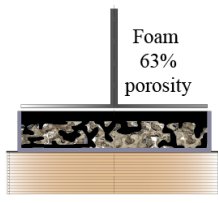

A controlled rate mode was used, with shear rates ranging between 1 and 50  $\text{s}^{-1}$ , and a test duration of 120 s. Samples were pre-sheared at 30  $\text{s}^{-1}$  during 60 s, and subsequently left to equilibrate under the action of the field during a further 60 s, before the application of the shear ramp. All experiments were conducted at 25  $\pm$  1 °C.



### Preparation of the magnetic foams

Four different foam-MRF preparations were studied, named A, B, C, and D, as described in Table 2. Sample A is the pure MRF, used for the sake of comparison. The maximum MR response is expected in this case. Samples C and D constitute the mixed systems, and they differ in the porosity of the metal foam (63 % and 69 %, respectively). Finally, we designate by B the sample consisting of MRF deposited on a solid aluminum piece. It can be considered as a contrast sample to ensure that any effects observed in C, D are not just the result of effectively reducing the cell gap, rather than the result of the foam-MRF synergistic behavior.

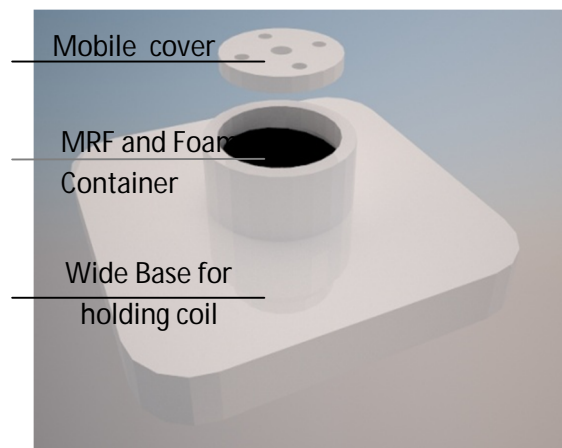
**Table 2.** Systems designation and exponent  $n$  of the power-law fitting of yield stress as a function of field strength with 45% v/v concentration. ( $\tau_y = m B^n$ ), for the samples indicated.

	A	B	C	D
System				
% of MRF	100	49.9	65.2	68.2
Vol. contained (mL)	5	2.47	3.26	3.41
Exponent, $n$	$2.3 \pm 0.1$	$0.9 \pm 0.1$	$1.5 \pm 0.1$	$1.6 \pm 0.1$

### Mechanical compressive analysis

In order to test the composites in somewhat realistic conditions, that is, when working under compression and not just under shear, we carried out a compressive

analysis by placing the magnetic foams in the home-made test cell depicted in Figure 3. A compressive stress was applied on top of the mobile cover using a SPECAC 25.011 (UK) manual press, capable of applying up to 15 T of force, or 1.43 MPa pressure. Both the spindle in the compressive machine and the cover of the device (shown in Figure 3) had a diameter of 2.54 cm. The magnetic field was applied by passing a current of up to 2.5 A along a coil surrounding the container (1270 turns, copper wire 0.7 mm in diameter); the highest magnetic field in the samples was 150 mT (in air). The MRF used for this evaluation was the one containing 45 % v/v concentration of solids.



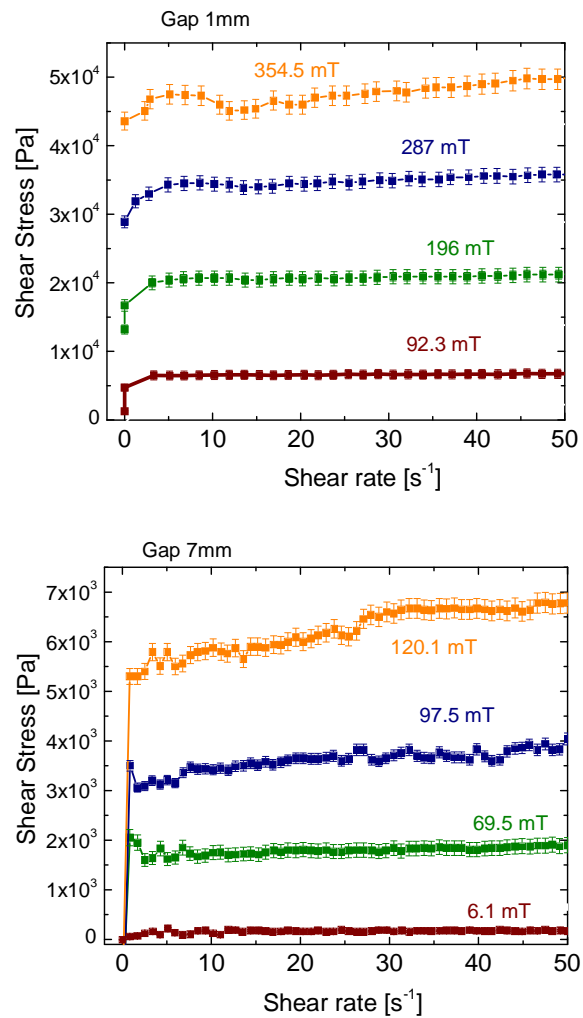
**Figure 3.** Cell used for the compression tests.

## RESULTS AND DISCUSSION

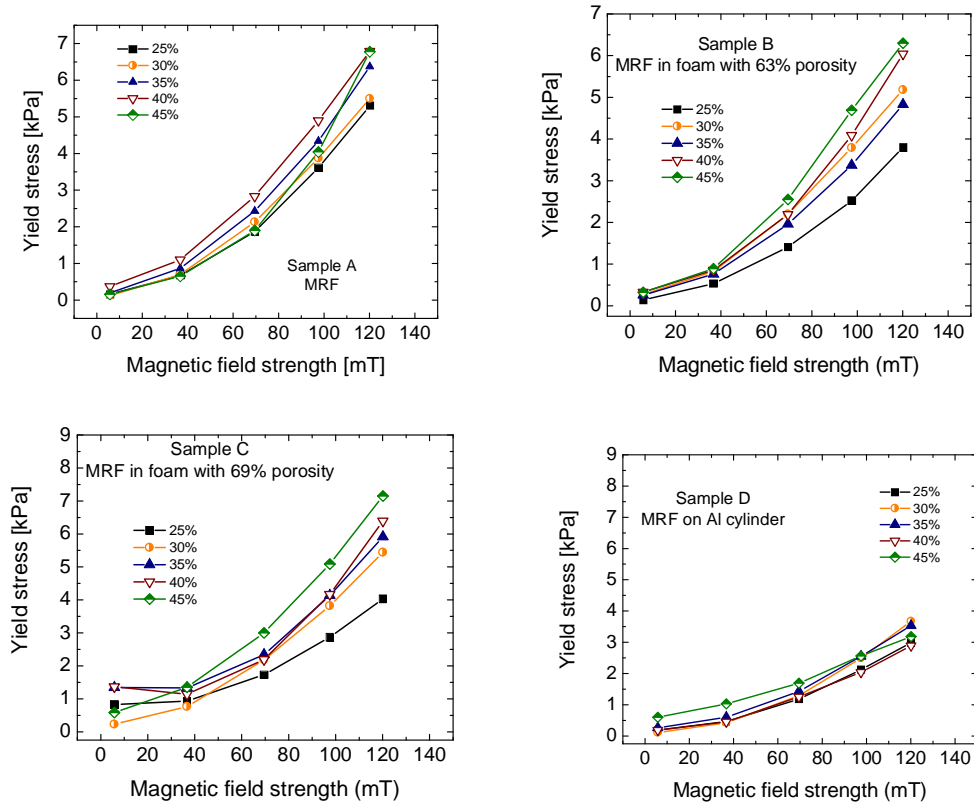
### *Magnetorheological analysis of the suspensions and magnetic foams*

Figure 4 shows typical rheograms for the pure MRF with 45% Fe, using two gaps, the ideal one (1 mm plate distance) and the one to be used when the foam is in the rheometer cell (7 mm). Note that the behaviors are similar in both cases, and the obvious difference that the maximum field attainable is smaller in the second case is the only observation worth to consider. A straightforward consequence of this fact is the reduction of the maximum shear stress for the same rate. Let us also point out that for the two experimental conditions the samples show yield stress increasing with the field strength. The yield stress was evaluated by fitting the rheograms to the Bingham equation (the so-called dynamic yield stress), and the results are presented in Fig. 5, in the form of yield stress  $\tau_y$  vs. magnetic field strength. Note that the field dependence of the yield stress is parabolic in the pure MRF, but the power exponent  $n$  of the fittings  $\tau_y = m B^n$  (Table 3) is smaller for the foam-MRF systems: the presence of the metallic

foam appears to hinder the formation of particle chains by dipolar interactions, which seem to be hindered by the confinement of the MR fluid.

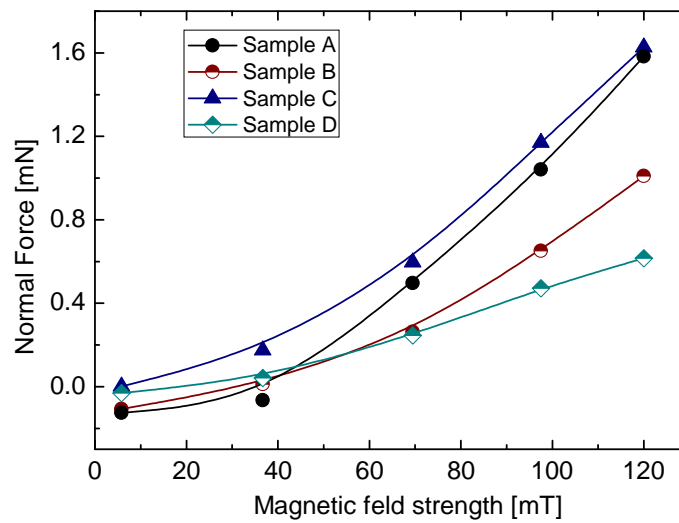


**Figure 4.** Shear stress as a function of shear rate for the 45 % MRF and cell gaps of 1 mm (top) and 7 mm (bottom).



**Figure 5.** Yield stress as a function of magnetic field strength for the MR fluid and 7 mm gap. (Sample type and iron concentrations are indicated in the figures).

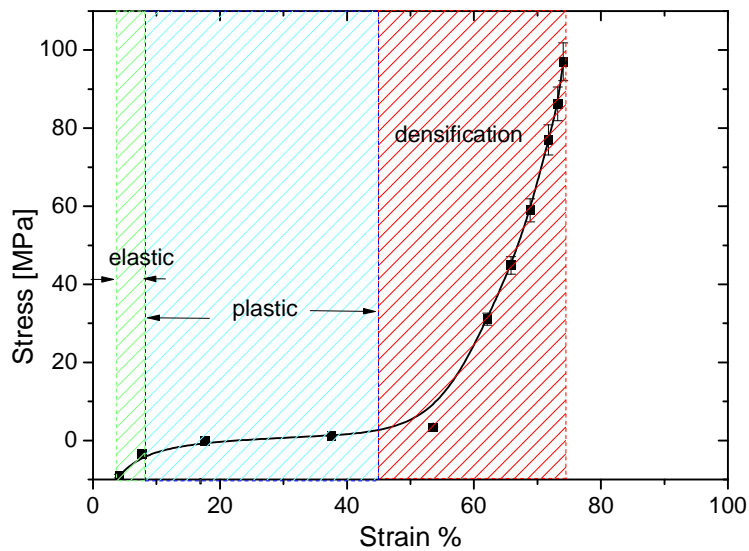
Normal force determinations were also carried out in all cases. The conclusions drawn on the shear stress results are largely confirmed in that kind of analysis, as Fig. 6 demonstrates for a typical situation ( $50 \text{ s}^{-1}$  shear rate, 45 % volume fraction of iron in the MRF). The best MR response corresponds to sample C (comparable or even better than the pure fluid). The decreased porosity of sample B and its absence in sample D reduce the synergy between the metal and fluid components.



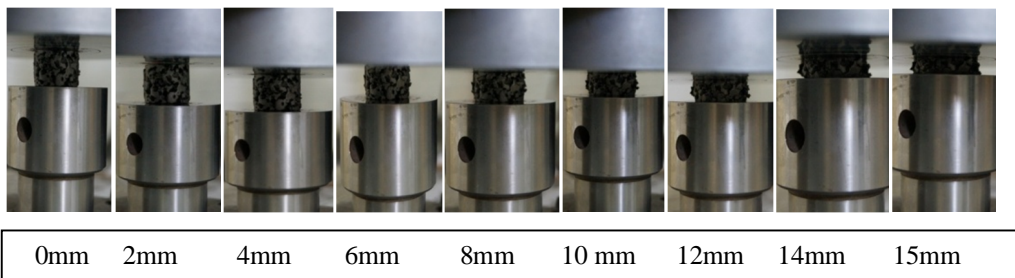
**Figure 6.** Normal force during the MR determinations detailed in Fig. 5, for samples A (MRF), B (MRF+63 % foam), C (MRF + 69 % foam) and D (MRF + Al cylinder). In all cases, the shear rate was  $50 \text{ s}^{-1}$ , and the concentration of iron particles was 45 %.

#### *Mechanical compressive analysis*

The strain of the aluminum foam normally displays three stages and it is expected that the magnetorheological fluid will be able to extend the first one, namely, elastic strain. The second and third ones, i.e., plastic deformation and densification (Fig.7), are not in the interest of this work. The whole test is illustrated by the pictures in Fig.8.



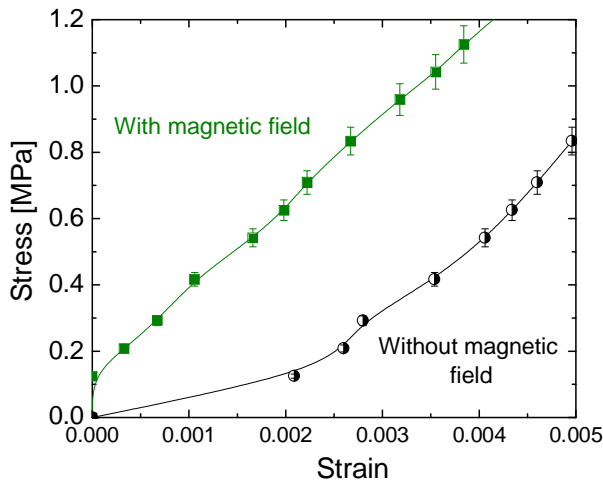
**Figure 7.** Compression test for an Al foam on the compression machine. Test tube:  $\varnothing 25.4$  mm, height 20 mm. Spindle speed 0.5 mm/min, and test load 8 Ton.



**Figure 8.** Photographs taken during the compression test of the aluminum foam .

The results of tests performed on type C (foam porosity 69% and 45% v/vMRF) MRF-foam composite with and without magnetic field are represented in Fig. 8. It can be observed that the magnetic field increases the resistance of the MRF-foam device to undergo deformation for given stress, a very significant result of this proof-of-concept investigation. This behavior can be justified based on the fact that the MRF-foam needs to be covered or enclosed so that the liquid cannot escape, when the magnetic field is OFF. However, if the magnetic field is applied, the state of aggregation of the MRF will be semisolid and the magnetorheological effect will try to prevent the densification of the foam, by forming the Fe chains oriented with the magnetic field. On the other hand, we have the compressive force that will try to break those chains leading to internal friction between both materials. The resulting balance, as Fig. 9 shows, indicates the

possibility of control of the mechanical behavior of the foam-MRF composite through magnetic field strength variations.



**Figure 9.** Compression test results, for sample C and 45 % v/v iron in the MRF.

## Conclusions

As a proof of concept of a magnetorheological damper, a composite system based on the combination of a metal (aluminum) foam and a magnetorheological fluid has been prepared and tested. Magnetorheological determinations confirm that the system behaves from the rheological point of view in a similar way as the pure magnetic fluid, except for a minor decrease in apparent the dynamic Bingham yield stress, but with the advantage of a much lower amount of fluid, necessary for filling the pores of the foam. The MR behavior is different from that found by the simple juxtaposition of an Al block and a fluid layer on top of it. This shows that the sought synergy takes place. This is even more clear in compression tests: the deformation for given pressure is considerably smaller in the foam-MRF system if the field is applied, precisely the final aim of this kind of devices. Although a very extensive investigation is still necessary, we believe that the idea is worth to be explored, since the two expected roles of these systems (magnetic field response and capacity to dissipate mechanical energy) appear to be present in the simple composites described.

**Acknowledgements**

Financial support was provided by projects PE2012-FQM694 (Junta de Andalucía, Spain), FIS2013-47666-C3-1-R (MINECO, Spain), SENER-CONACYT "151496" (UNAM Mexico), CONACYT National Quality Graduate Program. Support by National Autonomous University of Mexico (Mexico), Institute of Materials Research is also gratefully acknowledged.



## REFERENCES

- Banhart J (2001) Manufacture, characterisation and application of cellular metals and metal foams. *Progress in Materials Science* 46: 559-632.
- Baranwal D and Deshmukh TS (2008) MR-Fluid Technology and Its Application- A Review. *International Journal of Emerging Technology and Advanced Engineering* 2: 563-569.
- Bhatti AQ (2012) Performance of viscoelastic dampers (VED) under various temperatures and application of magnetorheological dampers (MRD) for seismic control of structures. *Mechanics of Time-Dependent Materials* 17: 275-284.
- Bossis G, Volkova O, Lacis S, et al. (2002) Magnetorheology: Fluids, Structures and Rheology. *Lecture Notes in Physics* 594: 202-230.
- Carlson JD (1999) Low-Cost MR fluid sponge devices. *Journal of Intelligent Material Systems and Structures* 10: 589-594.
- Carlson JD and Jolly MR (2000) MR fluid, foam and elastomer devices. *Mechatronics* 10: 555-569.
- Chacón-Hernando V (2009) Designing a suspension for a motor vehicle based on magneto-rheological dampers. PhD. Diss., Polytechnic School, University Carlos III, Madrid, Spain.
- de Vicente J, Klingenberg DJ and Hidalgo-Alvarez R (2011) Magnetorheological fluids: a review. *Soft Matter* 7: 3701-3710.
- Durán, JDG, González-Caballero F, Delgado AV, et al. (2008) Magnetorheological fluid. *Patent P200801895*, Spain.
- Eem SHH, Jung J and Koo JH (2013) Seismic performance evaluation of an MR elastomer-based smart base isolation system using real-time hybrid simulation. *Smart Materials and Structures* 22: 055003.
- Figuroa-Vargas IA, Lara-Rodriguez GA, Novelo-Peralta O, et al. (2012) Manual for production of metal foams by infiltration. Introduction and description of the production process by infiltration. National Autonomous University of Mexico, Institute of Materials Research, Mexico.

- Furst EM and Gast AP (2000) Micromechanics of magnetorheological suspensions. *Physical Review E* 61: 6732-6739.
- Fusheng H, Zhengang Z, Changsong L, et al. (1999) Damping behavior of foamed aluminum. *Metallurgical and Materials Transactions A* 30: 771-776.
- Gordaninejar F, Wang X, Hitchcock G, et al. (2010) *Modular High-Force Seismic Magneto-Rheological Fluid Damper*. *Journal of Structural Engineering* 136: 135-143.
- Gutiérrez-Vázquez JA and Oñoro J (2008) Review. Aluminum foams. Manufacture, properties and applications. *Revista de Metalurgia* 44: 457-476.
- Hosseini M, Farsangi EM (2012) Telescopic columns as a new base isolation system for vibration control of high-rise buildings. *Earthquakes and Structures* 3: 853-867.
- Liu XH (2010) Shear performance of novel disk-type porous foam metal magnetorheological (MR) fluid actuator. *Optoelectronics and Advanced Materials* 4: 1346-1349.
- Liu XH, Wong PL, Wang W, et al. (2010) Feasibility Study on the Storage of Magnetorheological Fluid Using Metal Foams. *Journal of Intelligent Material Systems and Structures* 21: 1193-1200.
- Lopez-Lopez M T, Kuzhir P, Lacis S, et al. (2006) Magnetorheology for suspensions of solid particles dispersed in ferrofluids. *Journal of Physics-Condensed Matter* 18: S2803-S2813.
- Park BJ, Fang FF and Choi HJ (2010) Magnetorheology: materials and application. *Soft Matter* 6: 5246-5253.
- Phulé PP, Mihalcin MP and Genc S (1999) The role of dispersed-phase remnant magnetization on the redispersibility of magnetorheological fluids. *Journal of Materials Research* 14: 3037-3041.
- Rodriguez-Arco L, Lopez-Lopez MT, Zubarev Ay, et al. (2014) Inverse magnetorheological fluids. *Soft Matter* 10: 6256-6265.
- Rossa C, Jaegy A, Lozada J, et al. (2014a) Design considerations for magnetorheological brakes. *IEEE-ASME Transactions on Mechatronics* 19: 1669-1680.
- Rossa C, Jaegy A, Micaelli A, et al. (2014b) Development of a Multilayerd wide-ranged torque magnetorheological brake. *Smart Materials and Structures* 23: 025028.

- Rudzka K, Viota JL, Munoz-Gamez JL, et al. (2013) Nanoengineering of doxorubicin delivery systems with functionalized maghemite nanoparticles. *Colloids and Surfaces B-Biointerfaces* 111: 88-96.
- Velte D, Jiménez I, Murillo N, et al. (2011) Foresight report on new smart materials. *FECYT, Spanish Foundation for Science and Technology*, Madrid.
- Yan YX, Hui LX, Yu M, et al. (2013) Dynamic response time of a metal foam magneto-rheological damper. *Smart Materials and Structures* 22: 025026.